PHYSICAL REVIEW E **89**, 041201(R) (2014)

High-order rogue waves in vector nonlinear Schrödinger equations

Liming Ling,[1] Boling Guo,[2] and Li-Chen Zhao[3,*]
[1]*Department of Mathematics, South China University of Technology, Guangzhou 510640, China*
[2]*Institute of Applied Physics and Computational Mathematics, Beijing 100088, China*
[3]*Department of Physics, Northeast University, Xi'an 710069, China*
(Received 18 January 2014; published 10 April 2014)

We study the dynamics of high-order rogue waves (RWs) in two-component coupled nonlinear Schrödinger equations. We find that four fundamental rogue waves can emerge from second-order vector RWs in the coupled system, in contrast to the high-order ones in single-component systems. The distribution shape can be quadrilateral, triangle, and line structures by varying the proper initial excitations given by the exact analytical solutions. The distribution pattern for vector RWs is more abundant than that for scalar rogue waves. Possibilities to observe these new patterns for rogue waves are discussed for a nonlinear fiber.

DOI: 10.1103/PhysRevE.89.041201 PACS number(s): 42.65.Tg, 05.45.Yv, 42.81.Dp

Introduction. Rogue wave (RW) is the name given by oceanographers to isolated large-amplitude waves which occur more frequently than expected for normal, Gaussian-distributed, statistical events [1–3]. It depicts a unique event that seems to appear from nowhere and disappear without a trace, and can appear in a variety of different contexts [4–7]. RWs have been observed experimentally in nonlinear optics [8,9], water wave tanks [10], and even in plasma systems [11]. These experimental studies suggest that the rational solutions of related dynamics equations can be used to describe these RW phenomena [12,13]. Moreover, there are many different pattern structures for high-order RWs [14–16], which can be understood as a nonlinear superposition of the fundamental RW (the first-order RW). Recently, many efforts were devoted to classifying the hierarchy for each order RW [17,18], since the superpositions are nontrivial and admit only a fixed number of elementary RWs in each high-order solution.

Recent studies were extended to RWs in multicomponent coupled systems, since complex systems usually involve more than one component [19–21]. For the coupled system, the usual coupled effects are cross-phase modulation. The linear stability analysis of the coupled system indicates that the cross-phase modulation term can vary the instability regime characters [22–24]. Moreover, for scalar systems, the velocity of the background field has no real effect on the pattern structure for RWs, since the corresponding solutions can be correlated through Galileo transformation. But for a coupled system, the relative velocity between different component fields has real physical effects, and cannot be erased by any trivial transformation. Therefore, the extended studies on vector RWs are nontrivial and meaningful. Recently, some novel patterns for RWs were presented in the coupled systems, such as dark RWs [25,26], the interaction between RWs and other nonlinear waves [26–28], a four-petaled flower structure [29,30], and so on. These studies indicate that there are very abundant pattern dynamics for RWs in the multicomponent coupled systems, which are quite distinctive from the ones in scalar systems.

Very recently, high-order RWs [31,32] were excited successfully in a water wave tank. This suggests that a high-order analytic RW solution is meaningful physically and can be realized experimentally [33]. However, as far as we know, the high-order vector RW has not been taken seriously until now. In [34], the authors consider the high-order RW solutions, which can be reduced into scalar ones, by a modified Darboux transformation (DT) method. As high-order scalar RWs are nontrivial superpositions of elementary RWs, the high-order vector ones could be nontrivial and possess more abundant dynamics characters. The knowledge about them would enrich our realization and understanding of RW complex dynamics.

In this Brief Report, we introduce a family of high-order rational solutions in a coupled nonlinear Schrödinger equation (CNLSE), which describes RW phenomena in multicomponent systems prototypically. We find that four fundamental RWs can emerge from the second-order vector RW in the coupled system, which is quite different from the scalar high-order ones for which it is impossible for four fundamental RWs to emerge. Moreover, six fundamental RWs can emerge in the distribution for the second-order vector RW.

The two-component coupled model. We begin with the well-known CNLSE in dimensionless form,

$$\begin{aligned} iq_{1,t} + q_{1,xx} + g(|q_1|^2 + |q_2|^2)q_1 = 0, \\ iq_{2,t} + q_{2,xx} + g(|q_1|^2 + |q_2|^2)q_2 = 0, \end{aligned} \tag{1}$$

where g is the nonlinear coefficient. The CNLSE model can describe the dynamics of matter waves in quasi-one-dimensional two-component Bose-Einstein condensate [20], the evolution of optical fields in a two-mode or polarized nonlinear fiber [21], and even the vector financial system [35]. With $g = 2$, Eq. (1) admits the following Lax pair:

$$\begin{aligned} \Phi_x &= (i\lambda\Lambda + Q)\Phi, \\ \Phi_t &= [3i\lambda^2\Lambda + 3\lambda Q + i\sigma_3(Q_x - Q^2)]\Phi, \end{aligned} \tag{2}$$

where

$$Q = \begin{pmatrix} 0 & q_1 & q_2 \\ -\bar{q}_1 & 0 & 0 \\ -\bar{q}_2 & 0 & 0 \end{pmatrix}, \quad \begin{aligned} \Lambda &= \mathrm{diag}(-2,1,1), \\ \sigma_3 &= \mathrm{diag}(1,-1,-1), \end{aligned}$$

the overbar represents complex conjugation. The compatibility condition $\Phi_{xt} = \Phi_{tx}$ gives the CNLSE (1).

*zhaolichen3@nwu.edu.cn

The standard DT [36] for linear system (2) is

$$\Phi[1] = T\Phi, \quad T = I + \frac{\bar{\lambda}_1 - \lambda_1}{\lambda - \bar{\lambda}_1}\frac{\Phi_1\Phi_1^\dagger}{\Phi_1^\dagger\Phi_1},$$
$$Q[1] = Q + i(\bar{\lambda}_1 - \lambda_1)[P_1, \Lambda], \tag{3}$$

where Φ_1 is a special solution for system (1) at $\lambda = \lambda_1$, and the symbol † represents the Hermitian transpose. It is well known that the standard N-fold DT should be done with different spectral parameters, or there will be some singularity in the DT matrix. The generalized DT was presented to solve this problem in [15], which can be used to derive high-order RWs conveniently by taking a special limit about the parameters λ_i.

The studies on the first-order vector RW in Refs. [26,28] indicate that there should be some restriction conditions on the plane-wave background fields ($\alpha_j \exp[ik_jx + w_jt]$, $j = 1,2$) to obtain the general RW solutions for CNLSE. The wave-vector difference of background plane wave $|k_1 - k_2|$ between the two components should satisfy certain relations with the background amplitudes α_j and nonlinear coefficient g, namely, $\alpha_1 = \alpha_2 = \alpha$ and $|k_1 - k_2| = \sqrt{\frac{g}{2}}\alpha$ [26]. In Ref. [28], they chose the seed solution

$$q_1 = \alpha e^{i(\frac{1}{2}\alpha x + \frac{15}{4}\alpha^2 t)}, \quad q_2 = \alpha e^{i(-\frac{1}{2}\alpha x + \frac{15}{4}\alpha^2 t)}.$$

In fact, the parameter α can be rescaled by scaling transformation. Thus we can consider a much simpler seed solution as the background where RWs exist without losing generality

$$q_1 = \exp\theta_1, \quad q_2 = \exp\theta_2, \tag{4}$$

where $\theta_1 = [i(\frac{1}{2}x + \frac{15}{4}t)]$ and $\theta_2 = [i(-\frac{1}{2}x + \frac{15}{4}t)]$.

We have proved that high-order RWs can be derived by taking a certain limit of the spectral parameter [15]. To take the limit conveniently, we set $\lambda_j = \frac{\sqrt{3}i}{2}(1 + \epsilon_j^3)$, $j = 1,2,\ldots,N$. Substituting seed solution (4) into Eq. (2), we can obtain the fundamental solution

$$\Phi_i(\lambda_j) = D\begin{bmatrix} \left[i\left(\lambda_j + \frac{1}{2}\right) - \xi_i\right]\left[i\left(\lambda_j - \frac{1}{2}\right) - \xi_i\right]\exp\omega_i \\ \left[i\left(\lambda_j - \frac{1}{2}\right) - \xi_i\right]\exp\omega_i \\ \left[i\left(\lambda_j + \frac{1}{2}\right) - \xi_i\right]\exp\omega_i \end{bmatrix},$$

where $i = 1,2,3$,

$$D = \mathrm{diag}(e^{\frac{5it}{2}}, e^{-\frac{i}{4}(2x+5t)}, e^{\frac{i}{4}(2x-5t)}),$$
$$\omega_i = \xi_i x + \left(i\xi_i^2 + 2\lambda_j\xi_i + 2i\lambda_j^2 + \frac{3i}{2}\right)t,$$

and ξ_i satisfies the following cubic equation:

$$\xi^3 - \left(\frac{9}{2}\epsilon_j^3 + \frac{9}{4}\epsilon_j^6\right)\xi - \frac{3}{2}\sqrt{3}\epsilon_j^3 - \frac{9}{4}\sqrt{3}\epsilon_j^6 - \frac{3}{4}\sqrt{3}\epsilon_j^9 = 0. \tag{5}$$

By the Taylor expansion of the fundamental solution form as done in [15], the generalized DT can be used to derive the RW solution. However, Taylor expansions of the fundamental solution form are quite complicated which results in very complex calculations. We find this process can be simplified greatly by the following special solution form:

$$\Psi_1(\lambda_j) = \frac{1}{3}[\Phi_1(\lambda_j) + \Phi_2(\lambda_j) + \Phi_3(\lambda_j)],$$
$$\Psi_2(\lambda_j) = \frac{\sqrt[3]{2}}{3\epsilon_j}[\Phi_1(\lambda_j) + \omega^2\Phi_2(\lambda_j) + \omega\Phi_3(\lambda_j)], \tag{6}$$
$$\Psi_3(\lambda_j) = \frac{\sqrt[3]{4}}{3\epsilon_j^2}[\Phi_1(\lambda_j) + \omega\Phi_2(\lambda_j) + \omega^2\Phi_3(\lambda_j)],$$

where $\omega = \exp[2i\pi/3]$, which are also the solution of the Lax pair with the seed solutions (4). We can prove that

$$\Psi(\epsilon_j) = f\Psi_1 + g\Psi_2 + h\Psi_3, \tag{7}$$

where

$$f = f_1 + f_2\epsilon_j^3 + f_3\epsilon_j^6 + \cdots + f_N\epsilon_j^{3(N-1)},$$
$$g = g_1 + g_2\epsilon_j^3 + g_3\epsilon_j^6 + \cdots + g_N\epsilon_j^{3(N-1)},$$
$$h = h_1 + h_2\epsilon_j^3 + h_3\epsilon_j^6 + \cdots + h_N\epsilon_j^{3(N-1)},$$

and f_i, g_i, and h_i are complex numbers, can be expanded around $\epsilon_j = 0$ with the following form:

$$\Psi(\epsilon_j) = \Psi^{[1]} + \Psi^{[2]}\epsilon_j^3 + \Psi^{[3]}\epsilon_j^6 + \cdots + \Psi^{[N]}\epsilon_j^{3(N-1)} + O\left(\epsilon_j^{3N}\right).$$

To obtain the vector RW solution, we merely need to take the limit $\epsilon_j \to 0$ [17]. After performing the generalized DT, we can present the Nth-order localized solution on the plane backgrounds with the same spectral parameter $\lambda_j = \frac{\sqrt{3}i}{2}(1 + \epsilon_j^3)$ as

$$q_1[N] = \exp\theta_1\frac{\det(M_1)}{\det(M)},$$
$$q_2[N] = \exp\theta_2\frac{\det(M_2)}{\det(M)}, \tag{8}$$

where

$$M_1 = M - 3iY_2^\dagger Y_1, \quad M_2 = M - 3iY_3^\dagger Y_1,$$
$$X = \begin{bmatrix} X_1 \\ X_2 \\ X_3 \end{bmatrix} = [\Psi^{[1]}, \Psi^{[2]}, \ldots, \Psi^{[N]}], \tag{9}$$

$Y_1 = X_1e^{-\frac{5it}{2}}$, $Y_2 = X_2e^{\frac{i}{4}(2x+5t)}$, $Y_3 = X_3e^{\frac{i}{4}(-2x+5t)}$, and $M = (M_{l,m})_{1\leqslant l,m\leqslant N}$. The $M_{l,m}$ can be derived by

$$\frac{\langle\Psi(\epsilon_j), \Psi(\epsilon_j)\rangle}{\lambda_j - \bar{\lambda}_j} = \sum_{l,m=1}^{+\infty,+\infty} M_{l,m}\epsilon_j^{3(m-1)}\bar{\epsilon}_j^{3(l-1)}.$$

The compact solution formula (8) can be used to derive an Nth-order RW solution. With $N = 1$, the first-order vector RW can be derived directly, which agrees well with the ones in [26,28]. We find the dynamics structures of high-order RWs in the coupled system are much more abundant than the ones in scalar systems [14–18]. Even for the second-order RWs, their distributions possess many different structures, which are quite different from the second-order scalar ones.

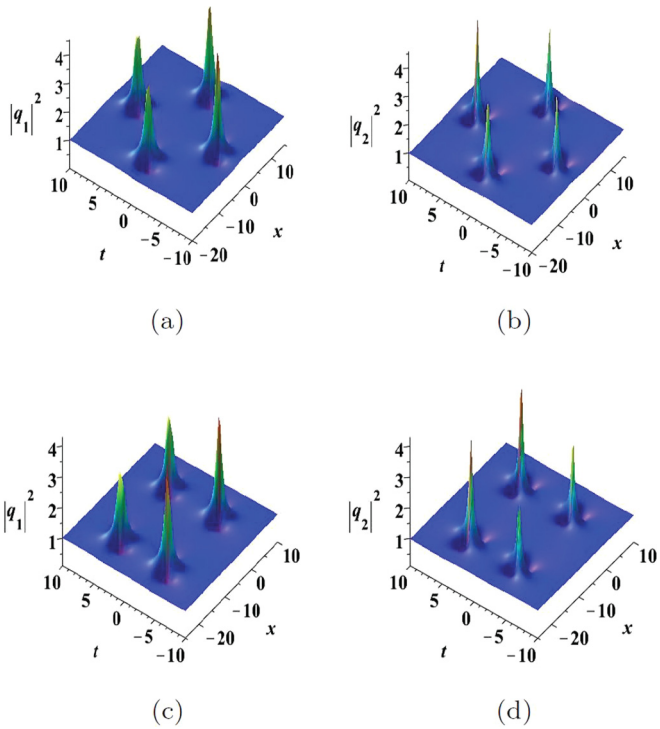

FIG. 1. (Color online) (a), (b) The rhombus structure for the second-order vector RW which contains four fundamental ones. The parameters are $f_1 = 0$, $f_2 = 0$, $g_1 = 1$, $g_2 = 0$, $h_1 = 0$, $h_2 = 10\,000$. (c), (d) The rectangle structure for the second-order vector RW which contains four fundamental ones. The parameters are $f_1 = 0$, $f_2 = 0$, $g_1 = 1$, $g_2 = 1000$, $h_1 = 10$, $h_2 = 0$.

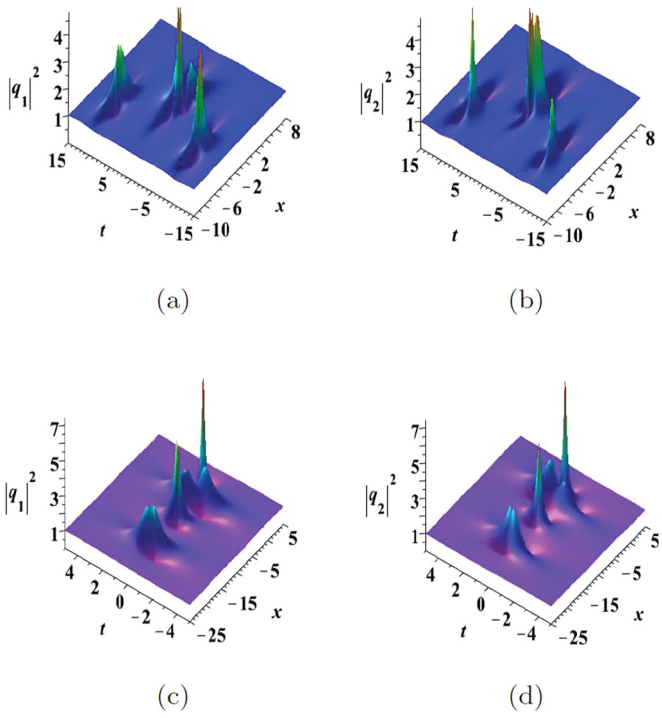

FIG. 2. (Color online) (a), (b) The triangle structure for the second-order vector RW which contains four fundamental ones. The parameters are $f_1 = 0$, $f_2 = 100$, $g_1 = 1$, $g_2 = 0$, $h_1 = 0$, $h_2 = 0$. (c), (d) The line structure for the second-order vector RW which contains four fundamental ones. The parameters are $f_1 = 0$, $f_2 = 0$, $g_1 = 1$, $g_2 = 0$, $h_1 = 10$, $h_2 = 0$.

As an example, we exhibit the dynamics behavior of a second-order vector RW solution. Since the expressions of the high-order RW solution are quite complicated, we will present them elsewhere.

The dynamics of second-order vector rogue waves. There are six free parameters in the generalized second-order RW solution, denoted by f_j, g_j, and h_j $(j = 1,2)$, which can be used to obtain different types or patterns for the rogue-wave dynamics. We find that there are mainly two kinds of RW solutions which correspond to four fundamental RWs and six fundamental ones obtained by setting $f_1 = 0$ and $f_1 \neq 0$, respectively.

First, we discuss the second-order RW solution which possesses four fundamental RWs. The pattern is quite different from the ones in a scalar NLSE system [17,18], for which it is impossible for four fundamental RWs to emerge on the temporal-spatial distribution plane. To obtain this kind of solution, we merely need to choose the parameter $f_1 = 0$. We classify them by parameters f_2, g_1, g_2, h_1, h_2 whether or not they are zeros. By this classification, there could be 2^5 kinds of different solutions which correspond to different patterns on the temporal-spatial distribution. We find there are mainly three types of the patterns, such as quadrilateral, triangle, and line structures.

The explicit shape of the quadrilateral can be varied through the parameters. As an example, we show two cases for the quadrilateral structure in Fig. 1. In the first case, the four RWs arrange with the rhombus structure [Figs. 1(a) and 1(b)]. The spatial-temporal distributions are similar globally in the two components, but the RW with the highest peak emerges at different times: it appears at time $t = -5$ for the component q_1, and at $t = 5$ for the component q_2. In the second case, the four RWs arrange with a rectangle structure [Figs. 1(c) and 1(d)]. It is seen that the peak values of the two RWs on the right-hand side are much higher than the ones on the left-hand side in the component q_1. The character is inverse for the component q_2.

Varying the other parameters, we can observe the interaction between the four RWs. When two of them fuse into a new RW, the three RWs can emerge with a triangle structure on the temporal-spatial distribution [Figs. 2(a) and 1(b)]. The structure of the triangle can be changed by varying the parameters. Especially, the three RWs can emerge into a line [Figs. 2(c) and 2(d)] which is perpendicular to the t axis. Namely, at a certain time, three or four RWs can emerge synchronously.

Second, we consider the second case of the second-order RW, which possesses six fundamental RWs. To obtain this kind of RW, we choose the parameter $f_1 = 1$. We find that the six fundamental RWs can constitute many different structures, such as pentagon, quadrilateral, triangle, and line structures. As an example, we show the pentagon structure in Figs. 3(a) and 3(b). The pentagon structure can be varied too by changing the parameters. There is one RW in the internal region of the pentagon, and its location in the

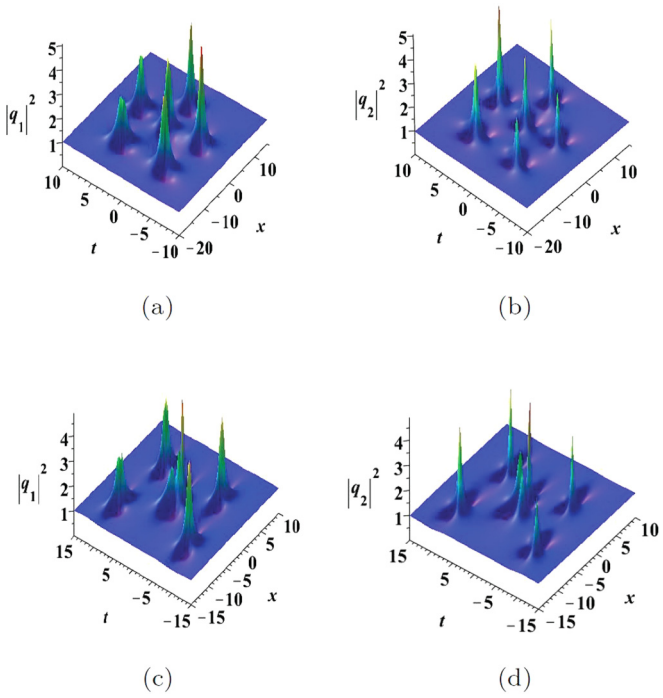

FIG. 3. (Color online) (a), (b) The pentagon structure for the second-order vector RW which contains six fundamental ones. The parameters are $f_1 = 1$, $f_2 = 0$, $g_1 = 0$, $g_2 = 0$, $h_1 = 0$, $h_2 = 10\,000$. (c), (d) The rectangle structure for the second-order vector RW which contains six fundamental ones. The parameters are $f_1 = 1$, $f_2 = 0$, $g_1 = 0$, $g_2 = 0$, $h_1 = 100$, $h_2 = 0$.

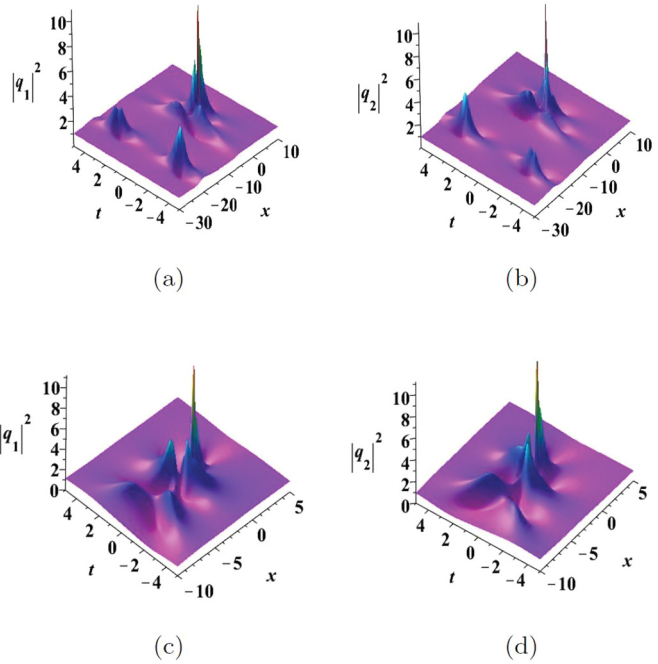

FIG. 4. (Color online) (a), (b) The triangle structure for the second-order vector RW which contains six fundamental ones. The parameters are $f_1 = 1$, $f_2 = 0$, $g_1 = 10$, $g_2 = 0$, $h_1 = 0$, $h_2 = 0$. (c), (d) The line structure for the second-order vector RW which contains six fundamental ones. The parameters are $f_1 = 1$, $f_2 = 0$, $g_1 = 0$, $g_2 = 0$, $h_1 = 0$, $h_2 = 0$.

distribution plane can be varied too. This case is similar to the pentagon structure of the third-order RW of a scalar NLS equation [17,18]. The six RWs can be arranged with the rectangle structure by varying the parameters, such as the one in Figs. 3(c) and 3(d). The structure is similar to the one in Figs. 1(c) and 1(d). But there is a new RW inside the rectangle, which is formed by the interaction of the other two fundamental RWs.

The six RWs can be also arranged with the triangle structure, shown in Figs. 4(a) and 4(b). In this case, there are two fundamental RWs and a new RW to form a triangle. The new RW is formed by the interaction between the other four fundamental RWs. Moreover, the RWs can be arranged with a line structure too, shown in Figs. 4(c) and 4(d). There should be six fundamental RWs arranged in one line case, but it is very complicated to derive the case since the parameters are too many to be managed well. We just show a particular one of the line cases.

Possibilities to observe these vector rogue waves. It is expected that these vector RWs could be observed in two-mode nonlinear fibers [8,9]. As an example, we consider the case that the operation wavelength of each mode is nearly 1.55 μm, the group-velocity dispersion (GVD) coefficients are -20 ps^2 km^{-1} in the anomalous regime, and the Kerr coefficients are nearly 1.1 W^{-1} km^{-1}, corresponding to the self-focusing effect in the fiber [37]. The unit in x direction will be denoted as 0.23 ps, and the one in t will be denoted as 0.55 km. One can introduce two distinct modes to the nonlinear fiber operating in the anomalous GVD regime [38,39]. The spontaneous development of RWs seeded from some perturbation should be on the continuous waves as those in [8,9]. The continuous-wave background intensities in the two modes should be equal (assume to be 1 W), and the frequency difference between the two modes should be 0.23 ps^{-1} to observe the vector RW. We can manipulate the initial perturbation approaching the ideal initial condition to observe these vector RW patterns. The ideal initial condition including intensity and phase profiles can be given by the exact second-order vector RW solution with given parameters in the scaled units. Moreover, the initial intensity and phase profiles can be made through the related modulation operator [9,37]. The vector RWs could be observed in the nonlinear fiber while approaching the ideal initial excitation form presented here [9].

Conclusions. We present a generalized RW solution of the CNLSE which can be used to obtain an arbitrary-order vector RW. We find that there are mainly two kinds of rogue-wave solutions for the second-order vector RW in CNLSE, which correspond to four fundamental RWs and six fundamental ones. Based on these results, we expect that there are many more abundant exotic patterns for RWs in NLSEs with three or more components.

Acknowledgments. This work is supported by the National Natural Science Foundation of China (Contract No. 11271052) and the Fundamental Research Funds for the Central Universities (Contract No. 2014ZB0034).

[1] M. Onorato, S. Residori, U. Bortolozzo, A. Montina, and F. T. Arecchi, Phys. Rep. **528**, 47 (2013).
[2] C. Kharif, E. Pelinovsky, and A. Slunyaev, *Rogue Waves in the Ocean* (Springer, Heidelberg, 2009).
[3] A. R. Osborne, *Nonlinear Ocean Waves and the Inverse Scattering Transform* (Elsevier, New York, 2010).
[4] V. Ruban, Y. Kodama, M. Ruderman *et al*., Eur. Phys. J. Special Topics **185**, 5 (2010).
[5] N. Akhmediev and E. Pelinovsky, Eur. Phys. J. ST **185**, 1 (2010).
[6] C. Kharif and E. Pelinovsky, Eur. J. Mech. B Fluid. **22**, 603 (2003).
[7] E. Pelinovsky and C. Kharif, *Extreme Ocean Waves* (Springer, Berlin, 2008).
[8] D. R. Solli, C. Ropers, P. Koonath, and B. Jalali, Nature **450**, 1054 (2007).
[9] B. Kibler, J. Fatome, C. Finot, G. Millot, F. Dias, G. Genty, N. Akhmediev, and J. M. Dudley, Nat. Phys. **6**, 790 (2010).
[10] A. Chabchoub, N. P. Hoffmann, and N. Akhmediev, Phys. Rev. Lett. **106**, 204502 (2011).
[11] H. Bailung, S. K. Sharma, and Y. Nakamura, Phys. Rev. Lett. **107**, 255005 (2011).
[12] A. R. Osborne, Mar. Struct. **14**, 275 (2001); N. Akhmediev, A. Ankiewicz, and M. Taki, Phys. Lett. A **373**, 675 (2009).
[13] N. Akhmediev, A. Ankiewicz, J. M. Soto-Crespo, and J. M. Dudley, Phys. Lett. A **375**, 541 (2011).
[14] Y. Ohta and J. K. Yang, Proc. R. Soc. A **468**, 1716 (2012).
[15] B. L. Guo, L. M. Ling, and Q. P. Liu, Phys. Rev. E **85**, 026607 (2012); Stud. Appl. Math. **130**, 317 (2013).
[16] J. S. He, H. R. Zhang, L. H. Wang, K. Porsezian, and A. S. Fokas, Phys. Rev. E **87**, 052914 (2013).
[17] L. M. Ling and L. C. Zhao, Phys. Rev. E **88**, 043201 (2013).
[18] D. J. Kedziora, A. Ankiewicz, and N. Akhmediev, Phys. Rev. E **88**, 013207 (2013).
[19] C. Becker, S. Stellmer, P. Soltan-Panahi, S. Dörscher, M. Baumert, E.-M. Richter, Jochen Kronjäger, K. Bongs, and K. Sengstock, Nat. Phys. **4**, 496 (2008).
[20] C. Hamner, J. J. Chang, P. Engels, and M. A. Hoefer, Phys. Rev. Lett. **106**, 065302 (2011).
[21] D. Y. Tang, H. Zhang, L. M. Zhao, and X. Wu, Phys. Rev. Lett. **101**, 153904 (2008).
[22] O. C. Wright and M. G. Forest, Physica D **141**, 104 (2000); M. G. Forest, S. P. Sheu, and P. C. Wright, Phys. Lett. A **266**, 24 (2000).
[23] M. G. Forest and O. C. Wright, Physica D **178**, 173 (2003).
[24] K. W. Chow, K. K. Y. Wong, and K. Lam, Phys. Lett. A **372**, 4596 (2008).
[25] Y. V. Bludov, V. V. Konotop, and N. Akhmediev, Eur. Phys. J. ST **185**, 169 (2010).
[26] L. C. Zhao and J. Liu, J. Opt. Soc. Am. B **29**, 3119 (2012).
[27] F. Baronio, A. Degasperis, M. Conforti, and S. Wabnitz, Phys. Rev. Lett. **109**, 044102 (2012).
[28] B. L. Guo and L. M. Ling, Chin. Phys. Lett. **28**, 110202 (2011).
[29] L. C. Zhao and J. Liu, Phys. Rev. E **87**, 013201 (2013).
[30] F. Baronio, M. Conforti, A. Degasperis, and S. Lombardo, Phys. Rev. Lett. **111**, 114101 (2013).
[31] A. Chabchoub and N. Akhmediev, Phys. Lett. A **377**, 2590 (2013).
[32] A. Chabchoub, N. Hoffmann, M. Onorato, A. Slunyaev, A. Sergeeva, E. Pelinovsky, and N. Akhmediev, Phys. Rev. E **86**, 056601 (2012).
[33] M. Erkintalo, K. Hammani, B. Kibler, C. Finot, N. Akhmediev, J. M. Dudley, and G. Genty, Phys. Rev. Lett. **107**, 253901 (2011).
[34] B.-G. Zhai, W.-G. Zhang, X.-L. Wang, and H.-Q. Zhang, Nonlinear Anal.: Real World Appl. **14**, 14 (2013).
[35] Z. Y. Yan, Phys. Lett. A **375**, 4274 (2011).
[36] V. B. Matveev and M. A. Salle, *Darboux Transformations and Solitons* (Springer-Verlag, Berlin, 1991).
[37] J. M. Dudley, G. Genty, F. Dias, B. Kibler, and N. Akhmediev, Opt. Express **17**, 21497 (2009).
[38] V. V. Afanasyev, Yu. S. Kivshar, V. V. Konotop, and V. N. Serkin, Opt. Lett. **14**, 805 (1989).
[39] T. Ueda and W. L. Kath, Phys. Rev. A **42**, 563 (1990).